

# Seismic damage in the Lagina sacred area on the Mugla Fault: a key point for the understanding of the obliquely situated faults of western Anatolia

Volkan Karabacak

Received: 27 June 2015 / Accepted: 14 September 2015 / Published online: 6 October 2015  
© Springer Science+Business Media Dordrecht 2015

**Abstract** The western Anatolia extension region consists of major E-W trending normal faults and numerous subsidiary faults aligned obliquely to major fault systems. In this paper, the NW-SE trending Mugla Fault was studied through an archaeoseismological analysis of the Lagina sacred area, which was supported by geological and geomorphological field evidence collected along the fault zone. The sacred area is cut by fractures that have caused extensive deformations and displacements in ruins along the fault. The orientations of collapsed columns, folding on the grounds, dilation, and tilting of the walls are systematic. The axes of the observed deformations are perpendicular to the Mugla Fault and could be related to coseismic effects. Although there are no historical records of a large earthquake on the Mugla Fault, the results of thermoluminescence and radiocarbon dating in the Lagina sacred area indicate that a large event occurred in the 4th *c.* AD or slightly later. Thus, considering the field evidence that has been collected along the Mugla Fault, it can be concluded that subsidiary faults aligned obliquely to major normal fault systems have strike-slip components and may be associated with a significant portion of the recent dynamics in western Anatolia.

**Keywords** Western Anatolia · Archaeoseismology · Earthquake faulting · Lagina

## 1 Introduction

Western Anatolia is one of the most seismically active extensional regions in the world, primarily characterized by nearly N-S stretching (Şengör et al. 1985) (Fig. 1a). The most important features of this extension are E-W trending normal fault systems (i.e., the Büyük Menderes and Gediz Grabens) (Fig. 1a). Furthermore, there are numerous subsidiary faults representing strike-slip components aligned obliquely to major normal fault systems (i.e., the Söke and Seferihisar Faults aligned obliquely to the Büyük Menderes and Gediz Grabens, respectively). Although most of these faults are associated with instrumental earthquakes (Tan et al. 2008), their characteristic features and recent behaviors are still under debate (Uzel et al. 2012; Sümer et al. 2013). So far, these subsidiary faults are not as well documented as the neighboring major active faults, although it could be important for a better understanding of the extension dynamics in western Anatolia.

The Mugla Fault is a NW-SE trending fault zone, and it is obliquely situated slightly NE of the Gökova normal fault system, which has well-documented high earthquake potential (Fig. 1b). According to instrumental records (Tan et al. 2008), there have also been several minor to moderate earthquakes along this obliquely situated zone since the beginning of the twentieth century. For example, several strong ( $M_s > 6$ ) earthquakes

---

V. Karabacak (✉)  
Department of Geology, Eskisehir Osmangazi University,  
26480 Eskişehir, Turkey  
e-mail: karabacak@ogu.edu.tr

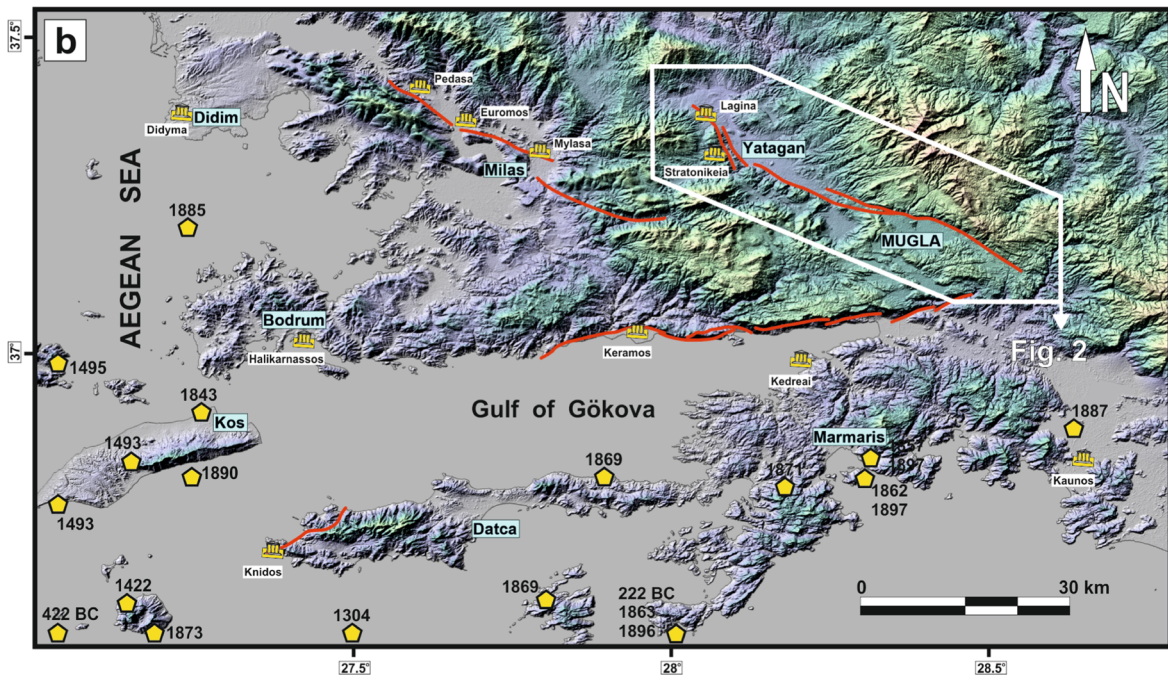
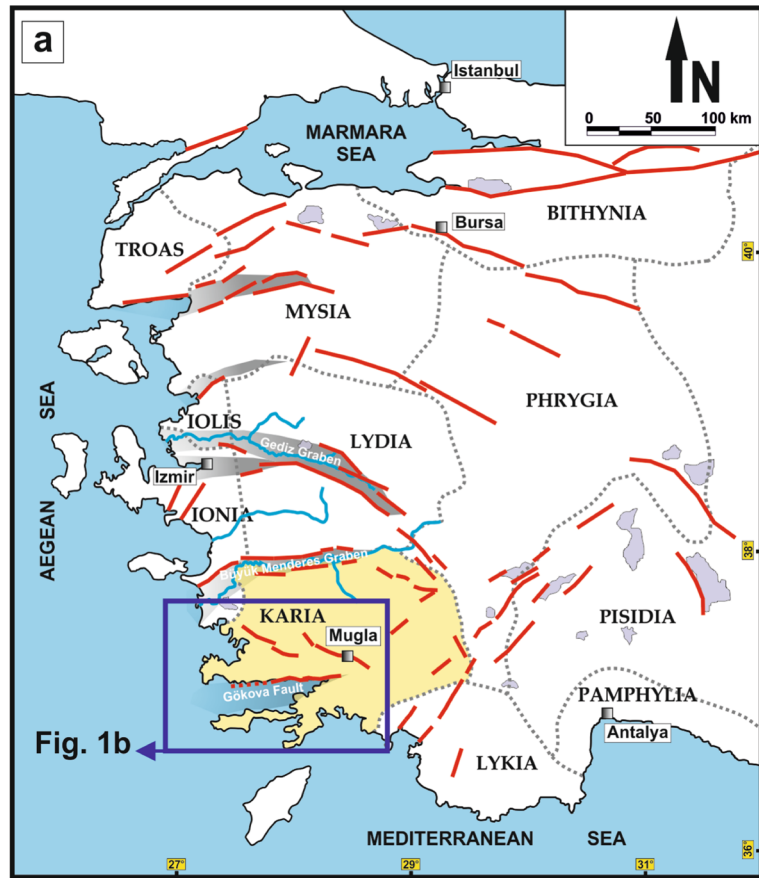


**Fig. 1** a Ancient regions of the Roman period and major active faults (red lines) in western Anatolia. b Major ancient settlements of the Karia region and historical earthquakes (relief is generated using the AsterGDEMv2 digital data) (historical earthquakes are taken from Tan et al. 2008)

occurred in 1941 and 1944 west of Mugla settlement (Fig. 2). This zone was first defined as an active fault by Şaroğlu et al. (1987). They called the fault the Mugla-Yatagan Fault Zone, which is thought to represent a regionally important zone and is mapped as a right-lateral strike-slip fault. Barka et al. (1996) characterized this zone on the east side of Mugla as a normal fault. They indicated that this zone is old and that there has been no earthquake activity for a long time. However, Eyidoğan et al. (1996), who investigated microearthquake activity in the Mugla region, noted a cluster of seismicity slightly west of Yatagan. These data confirm the activity of the Mugla Fault. Recently, based on kinematic analyses, Kahraman et al. (2011) suggest that E-W and NW-SE trending normal faults along the southwestern margin of the Yatagan plain are syn-extensional structures produced by the recent tectonic regime. The most recent fault map for the region indicates Mugla Fault as an active normal fault that ruptured in the Holocene (Duman et al. 2011). Thus, as indicated from previous studies, there is agreement on the existence of a NW-SE trending fault along the Mugla and Yatagan plains, but the sense of the motion and activity of the fault remain an open question in the western Anatolia extensional region.

The location of the Mugla Fault in the center of the Karia region, where there have been several established ancient settlements through ages, provides excellent opportunities for the interpretation of the fault’s seismic history (Fig. 1a). There are several records about previous strong earthquakes that occurred in the Karia region (e.g., in 227 BC, 199–198 BC, 142–144 AD, and 365 AD) that have caused damage in major ancient settlements such as Stratonikeia (Ergin et al. 1967; Soysal et al. 1981; Ambraseys and Finkel 1987; Guidoboni et al. 1994; Ambraseys and Jackson 1998; Guidoboni and Comastri 2005) (Fig. 1b). Some of these historical earthquakes seem to have been large enough to create surface faulting that could leave traces along the fault zones. Furthermore, the current locations and disposition of available ruins of ancient man-made structures in the Karia region would likely provide evidence of the historical earthquake activity.

Lagina located on the Mugla Fault was an important sacred area of the Roman era (Figs. 1b and 2) and, nowadays, presents well-preserved ruins; thus, studying the fault’s archaeoseismological potential may play a

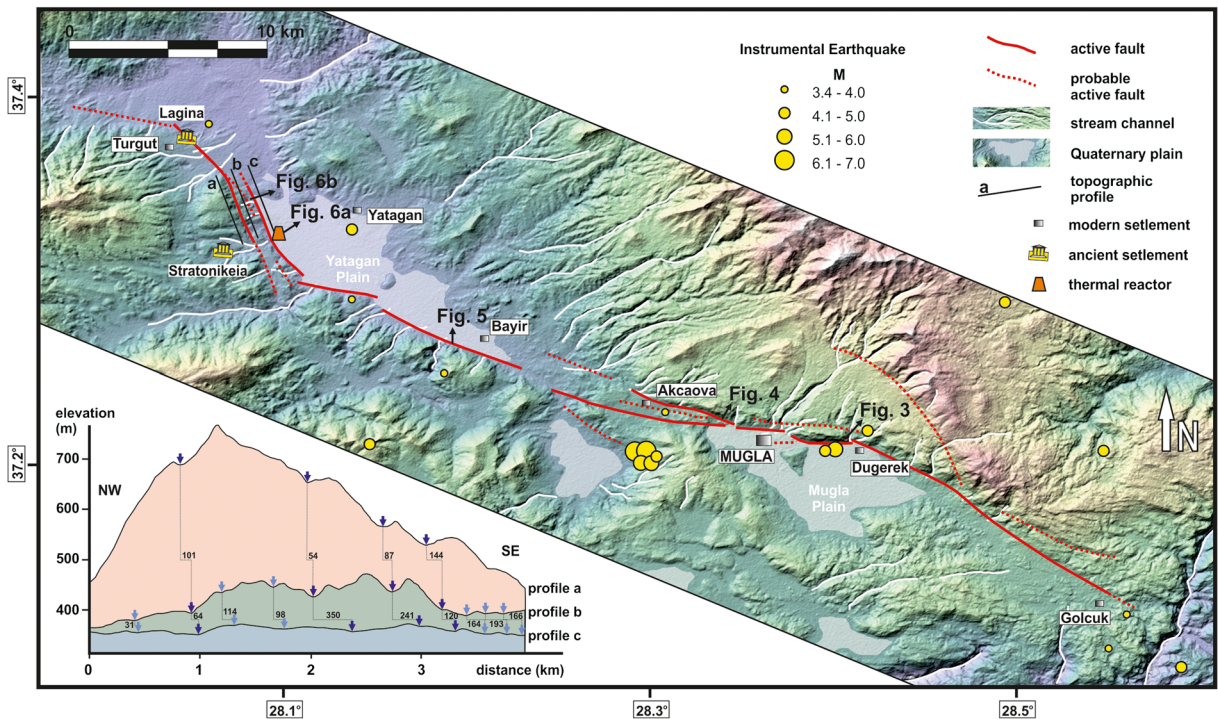


**Fig. 2** Shaded relief map of the study area (it is generated using the AsterGDEMv2 digital data). Note that *inset* section shows fault-parallel topographic profiles from the sides of fault branches (red lines show the fault; instrumental earthquakes are taken from Tan et al. 2008)

key role in understanding the recent fault behavior. In this study, detailed geological and geomorphological field observations are presented along the Mugla Fault to evaluate its characteristics. Furthermore, in terms of earthquake faulting, extraordinary archaeoseismological observations in the Lagina sacred area are revealed.

## 2 The Mugla Fault

The Mugla Fault extends in NW-SE direction in the Karia region of western Anatolia. As shown in Fig. 2, the actively filling Mugla plain is located on the southern side of the fault. The Mugla Fault does not provide clear evidence for active faulting east of Gölcük; thus, it was mapped as an inferred fault in this part. It exhibits a distinct morphology in the vicinity of the Dugerek (Fig. 3a). Further west, the fault roughly trends E-W toward the Mugla city center and bounds the northern margin of the Mugla plain (Figs. 2 and 3b). Along this margin, a high topographic escarpment exhibits clear evidence of dip-slip faulting (Fig. 3b).

Although fault planes are not well preserved in the unconsolidated units, fault morphology is visible in west of Mugla city (Fig. 4a). Nearly vertical planes are exposed along this morphology (Fig. 4b). A road cut crosses this morphological scarp, and it exposes faulted colluvium deposits (Fig. 4c). Sequencing of pebbles indicates shear zone, when vertical displacement on lower limit of colluvium shows normal motion on fault plane (Fig. 4c).

The slope of the Mugla plain gently decreases to the west, and it connects to the Yatagan plain to the northwest through Akcaova. Toward west, the fault displays a normal fault morphology in which the northern block has moved down (Fig. 5a). Obliquely, slickensides

along the scarp show evidence of dip-slip-dominant motion with a dextral strike-slip component (Fig. 5b). Further west of Bayir, the fault enters the Yatagan plain and it extends along the southwestern side of the plain (Fig. 2). The Yatagan plain is one of the western Anatolian Neogene depressions (Alcicek 2010). The sedimentary succession in the basin was first described and dated by Becker-Platen (1970), who considered it to be a single formation and divided it into the Turgut, Sekköy, Yatagan, and Milet members. Basement rocks composed of Paleozoic metamorphic schists and marble exhibit high topographic escarpments along the southwestern margin of the plain (Kahraman et al. 2011). The general morphology of the fault is characterized by linear topography between the plain and the escarpments. The Late Quaternary tectonic activity of this strand is characterized by faulted alluvial and colluvial deposits, triangulated faces, and dextrally offset streams. Mapping of the fault showed that it extends with right-stepping geometry.

West of Yatagan, the fault extends as two parallel branches in a direction of N 40° W near a thermal reactor (Figs. 2 and 6). Three fault-parallel topographic sections from the sides of both branches exhibit geomorphologic evidence of the active faulting geometry (Fig. 2). The topographic sections show that there are vertical displacements up to 300 and 100 m on the western branch and eastern branch, respectively (inset section in Fig. 2). Similar stream channel geometry on each block indicates that right-lateral displacements reach up to 144 and 350 m on the western branch and eastern branch, respectively. Furthermore, both fault branches cut four stream channels where cumulative offsets reach up to 404 m (inset section in Fig. 2). Thus, considering cumulative vertical and lateral

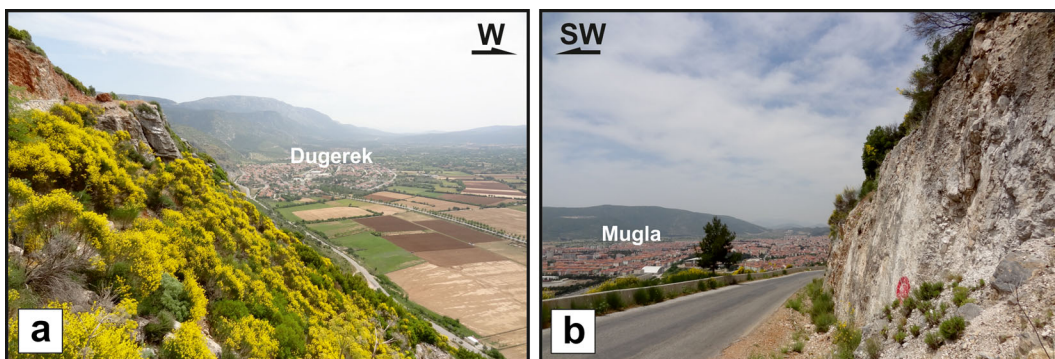


**Fig. 3** **a** Distinct normal fault morphology in the vicinity of the Dugerek. **b** A view of the Mugla fault in the Mugla city center (for location, see Fig. 2)

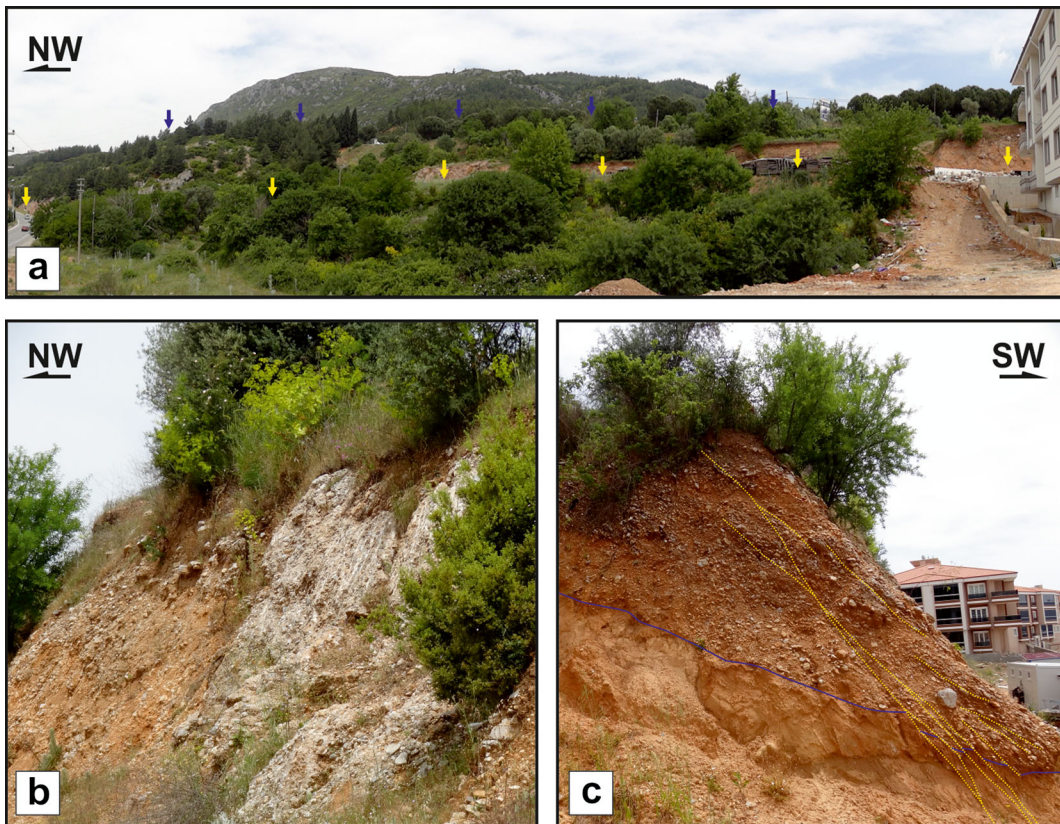


**Fig. 4** **a** A general view from the western entrance of the Mugla city (*blue and yellow arrows* show two parallel branches of the fault). **b** A semi-protected fault scarp along the southern branch that

is indicated with *yellow arrows* in **a**. **c** Faulted colluvium deposits on road cut that cross this morphological scarp (for location, see Fig. 2)

displacements, it can be concluded that the fault has a dip-slip and strike-slip in almost equal proportions.

Further northwest, the branches of the Mugla Fault join and it extends as a single fault in pre-Quaternary rock units (Fig. 2). The Miocene-Pliocene lacustrine

units crop out in this area (Kahraman et al. 2011). They are well bedded, and they mainly consist of sandy silt, clay, and lignite layers (Gürer et al. 2011). East of Turgut, the fault can be traced by fault-related linear topography and offset stream beds. The fault turns

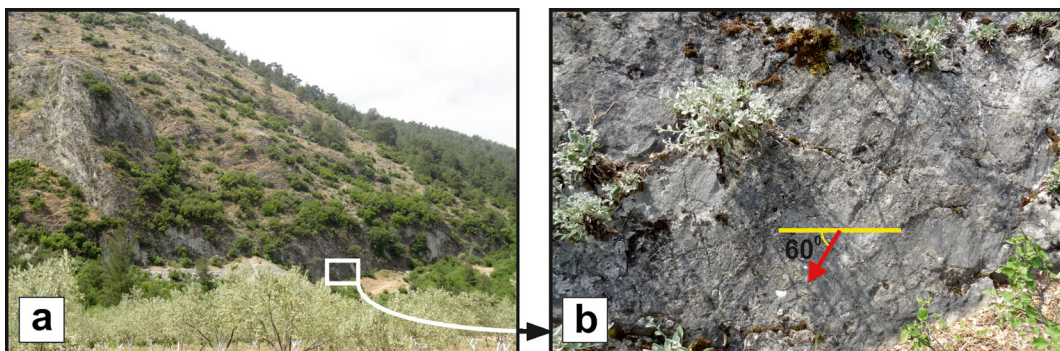


**Fig. 5** **a** A general view of the fault from the south of Bayir. **b** Obliquely slickensides on the limestones indicate dip-slip motion with strike-slip component in this area (for location, see Fig. 2)

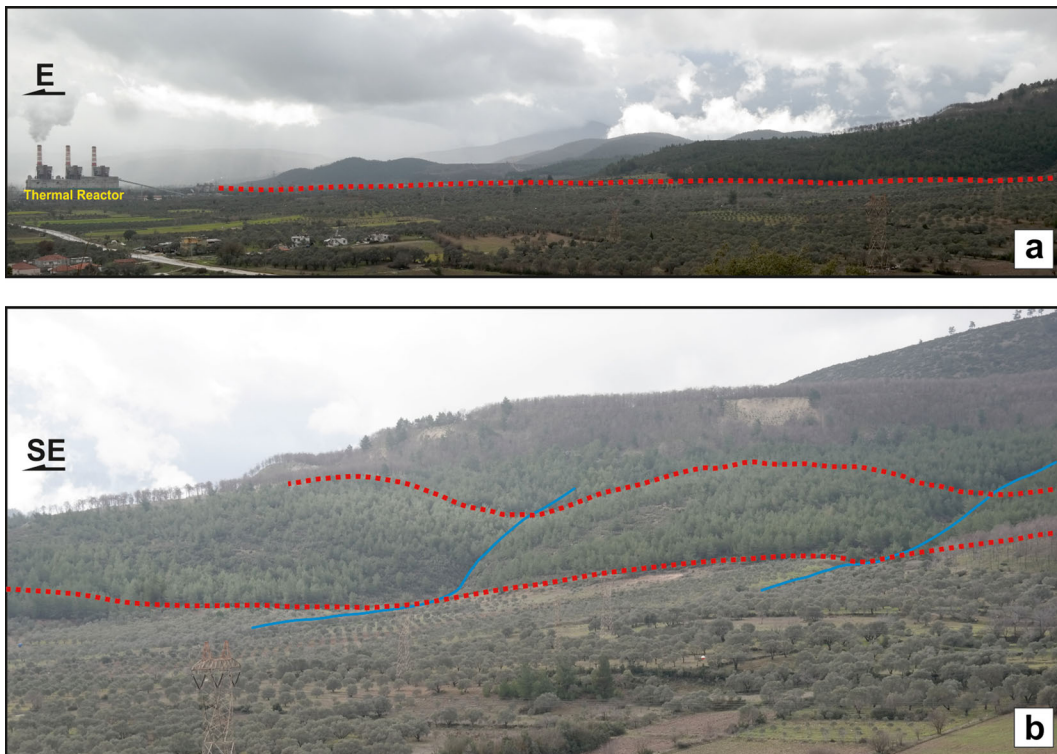


**Fig. 6** **a** A general view from the Mugla Fault (*red dashed lines* show the trace of the fault in the field). **b** Two parallel branches of the fault northwest of the thermal reactor (*blue lines* show left-laterally displaced stream beds) (for location, see Fig. 2)

toward the WNW, and it does not provide clear evidence for faulting further west; thus, it was mapped as a probable fault in this part.

### 3 Archaeoseismological potential of Lagina

The Lagina sacred area is located on a low-sloping open land along the Mugla Fault in the Karia region of the ancient world (Figs. 2 and 7a). Although the detailed history of Lagina is not as well known as other major ancient cities of the Karia, it has been documented that the sacred area was initially established in approximately the 8th c. BC along with an increasing number of new settlements surrounding it. Lagina became part of the ancient city of Stratonikeia, and it began to develop during the second half of the 3rd c. BC (Büyükozer 2010; Ekici 2010). The sacred area suffered from plundering in the last half of the 1st c. BC, and the damage was offset with the assistance of the emperor Augustus (Tirpan 1997).

Lagina maintained its importance during the Roman and early Byzantine eras and was decorated with

monumental architectural buildings of compact structure (Ekici 2010). It was composed of several types of buildings, such as a propylon, altar, stoa, temple, and a chapel (Fig. 7b). All structures except the chapel were completed during the Emperor Augustus period (27 BC) at the latest. It has been documented that there were destruction and rebuilding in the sacred area during the 2nd c. AD, especially in the stoa. Finally, the last monumental building, the chapel, was built in 325 AD (Tirpan and Söğüt 2010). Based on archaeological evidence from coins found in the area, it has been concluded that the entire area became unusable after the buildings in Lagina collapsed as the result of an earthquake in the last half of the 4th c. AD (Tirpan and Söğüt 2003; Tirpan 2012). Systematic excavations at Lagina that begun in 1993 under the direction of Prof. A. A. Tirpan have exposed large parts of the ruins. Although all the major buildings partly collapsed, their associated ruins were well preserved as a result of being buried.

Detailed field investigations during this study have indicated that structures of the Lagina sacred area may have been affected by the earthquake damage. Evidence

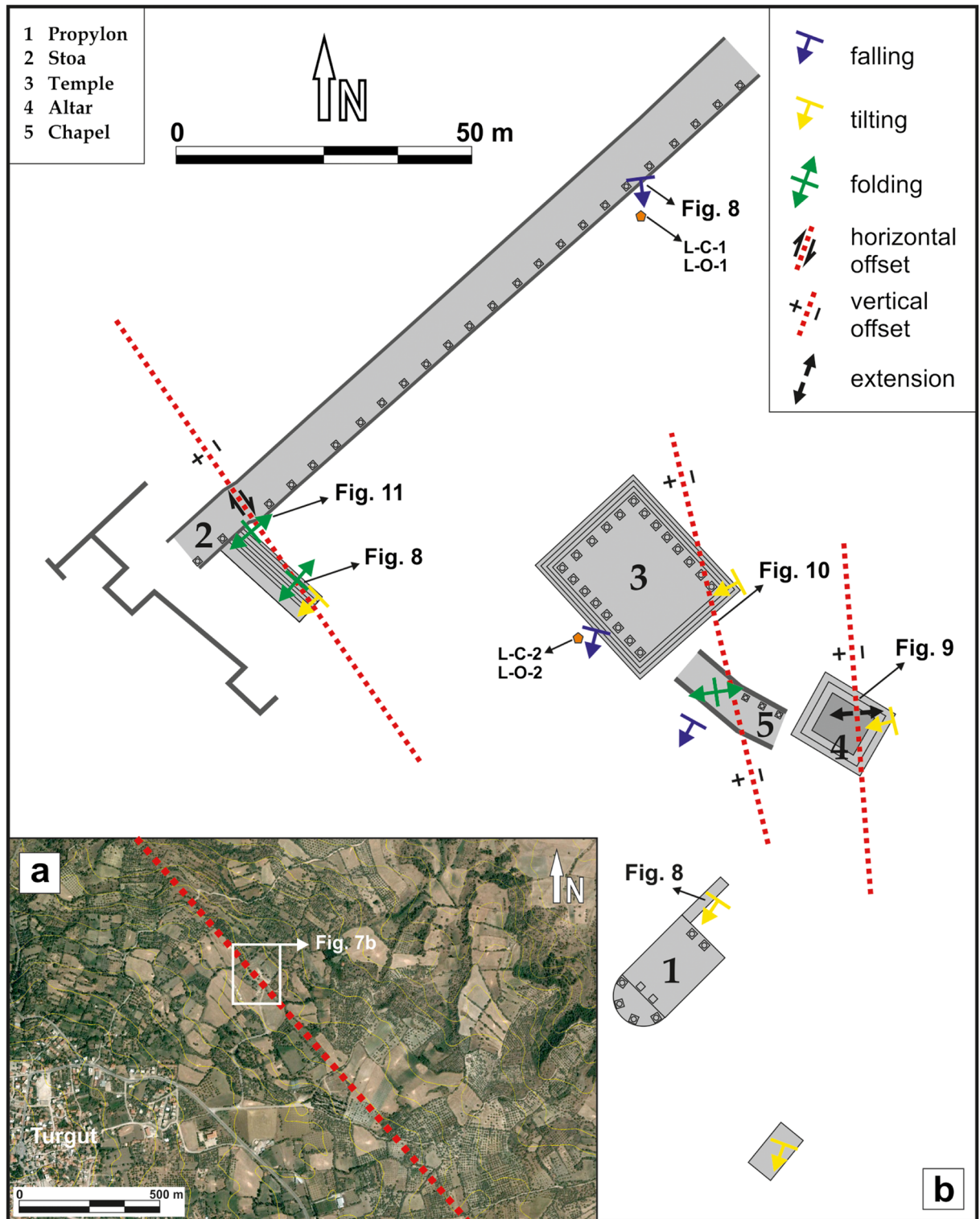
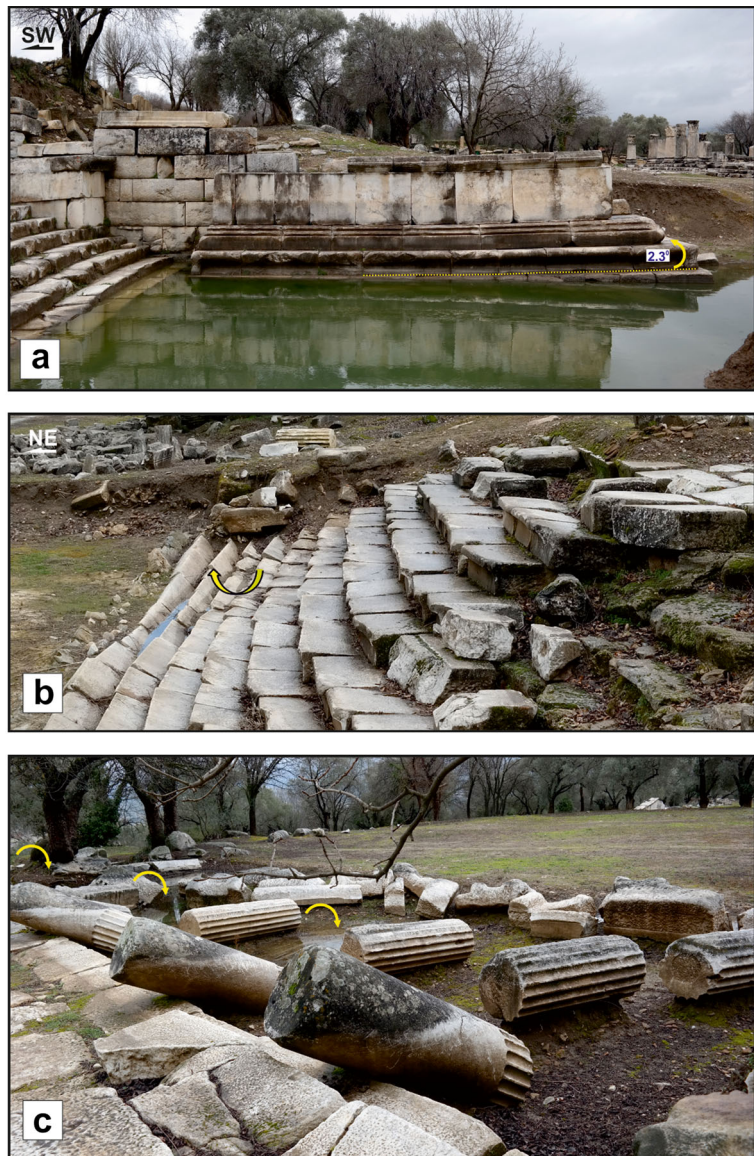


**Fig. 7** **a** Satellite image of the Lagina sacred area and its surroundings (taken from Google Earth). *Yellow lines* indicate topographic isohypse curves at 10-m intervals. **b** The plan of the Lagina sacred area main buildings and archaeoseismological indicators

**Fig. 8** **a** Tilted wall of the Propylon in Lagina. **b** Folding on steps of the stoa along the fault. **c** Parallel fallen side columns of the stoa area. Note that *horizontal trace* that indicates archaeological excavations revealed a series of parallel fallen columns (for location, see Fig. 7)



of seismic deformation of the ruins is characterized by, in particular, tilting and rotation of blocks, falling of oriented columns, and remains folded and faulted. For example, some of the remaining walls and ground floors are tilted toward the southwest approximately  $2\text{--}8^\circ$  (i.e., Figs. 7b and 8a). The altar was split diagonally in the middle (Fig. 7b), and the western half of the altar was displaced downward approximately 40 cm with tilting (Fig. 6a). There is evidence of a notable NNW-trending rupture that dilated blocks up to 50 cm (Fig. 9b). Similarly, the western corner of the temple was also interrupted in a NNW-trending zone (Fig. 7b). The western side of this zone

was upthrown approximately 55 cm relative to the other side of the zone (Fig. 10). There is also evidence of folding and “pop-up” deformations along the extension of this zone at the base blocks of the temple and chapel (Fig. 10).

The most noteworthy evidence of earthquake faulting was observed at the entrance of the stoa (Fig. 7b). The columned sidewalls were ruptured by a NW-SE trending dextral fault (Fig. 11). The southeastern margin wall is displaced right-laterally approximately 1 m solely within this zone (Figs. 7b and 11). A small pond was tilted, and steps of the stoa were prominently folded along the rupture (Figs. 8b and 11).



**Fig. 9** **a** Deformation on the western half of the altar. *Red arrows* show the fault. **b** The NNW-trending rupture on the altar that splits it in the middle diagonally. *Yellow arrows* indicate dilatation directions (for location, see Fig. 7)



Most side columns at the Lagina sacred area fell in a parallel pattern. For example, the new archaeological excavations at the stoa area near the temple and the chapel revealed a series of fallen columns. The fallen columns are systematically aligned in S-SW direction (Figs. 7b and 8c). Although recent studies based on analog and numerical modeling assert that the

relationship between strong ground motion and the effects on manufacts is not entirely linear (e.g., Hinzen 2009), parallel fallen columns are common diagnostic indicators of archaeoseismic deformation (e.g., Stiros 1996; Marco et al. 2008; Karabacak et al. 2013). Thus, it is important to know the time of collapse of the fallen columns, which could indicate coseismic shaking



**Fig. 10** Faulting along the temple and chapel. *Red arrows* show the fault (for location, see Fig. 7)

**Fig. 11** Right-lateral offset on the southeastern margin wall of the stoa. Note that a small pond within the zone was also tilted. Red arrows show the fault (for location, see Fig. 7)



damage, to date historical earthquake in Lagina. The surface soils were covered by the collapsed columns due to earthquake shaking. Following the collapse of the columns, the surface soils were buried by subsequent sediment deposition, which preserved the contents within the buried surface soils, such as charcoal, bone, and ceramics. Radiocarbon dating method was used to document the age of deposits that were buried following the systematic column collapses and determine the lower limit of the time of collapse and related earthquakes. Exposed sediment deposits were carefully scraped from beneath the two individual columns, which allowed access to the undisturbed sampling site. Ceramic pieces in buried material were taken to thermoluminescence (TL) dating as well as radiocarbon samples from each location. Figure 7b depicts the locations where the samples were taken. The measured radiocarbon and TL ages are summarized in Table 1.

#### 4 Discussion

Geological and geomorphological field data indicate that the Mugla Fault is approximately 60 km in length. It has a normal fault character in which the opposite block has moved down on both ends. Dextrally deflected stream beds and obliquely slickensides on the scarps are characteristic evidences for the right-lateral component along the Mugla Fault. Offsets on the young stream channels

and fault-controlled Quaternary basins clarify the activity of the Mugla Fault.

Field observations in the Lagina sacred area indicated extensive damage characterized by faulting, collapsed columns, dilated ruptures, folding, and tilted walls. The orientations of the collapsed columns, folding on the grounds, dilation, and tilting of the walls are systematic, and the axes of these deformations are perpendicular to the Mugla Fault. Such phenomena are characteristic criteria for archaeoseismological studies (e.g., Karcz and Kafri 1978; Stiros 1996; Galadini et al. 2006; Marco et al. 2008; Bottari et al. 2009) and can be attributed to the strong ground shaking. Thus, this extensive systematic destruction may be associated with historical earthquake or earthquakes that struck the sacred area from same source.

Lagina was cut by three NW-trending ruptures that caused extensive deformations and displacements in the structures' ruins. There are two plausible interpretations regarding the origin of these ruptures in the sacred area. (1) An earthquake occurred in the proximity of the region with a considerable intensity, was responsible for the observed destruction, and triggered a mass movement around Lagina. If this is the case, downward displacements with tilting and dilation of the altar and the temple are postulated to be a result of a landslide in the sacred area. (2) The source of the ruptures may be earthquake faulting on the Mugla Fault. If this is the case, the combined surface observations of the altar, temple, and stoa indicate that the sacred area was in a transtensional fault zone and that the resulting deformation was of tectonic origin. Thus, this

**Table 1** TL and radiocarbon dating results

Sample	Material	Measured age	Conventional age	2 Sigma calibration	Calibrated age result (68 % probability)
L-C-1	Bone collagen (collagen extraction with alkali)	1600±30 BP	1790±30 BP	AD 135–265 and AD 275–330	AD 220–255 AD 300–315
L-C-2	Organic sediment (acid washes)	1630±30 BP	1640±30 BP	AD 345–430 and AD 490–530	AD 405
Sample	Material	Depth (cm)	Dose (Gy)	Dose rate (Gy/ka)	Calculated age result
L-O-1	Ceramic	105	10100±300	4950±300	BC 285–AD 315
L-O-2	Ceramic	90	9500±200	4950±290	AD 15–215

fault extension should be investigated as part of paleoseismological studies to better understand its recurrence time.

The geological characteristic of the site is important criteria for evaluating that the observed deformation reflects a direct tectonic effect or a secondary ground deformation. Sometimes, a notable earthquake in the proximity of the region could trigger a mass movement on unconsolidated units (Keefer 1984). However, the geological background of the studied site at the Lagina indicates that it is an area located on consolidated well-bedded units and covered with Holocene deposit which does not exceed 1 m (Fig. 12). Considering the physiography indicated by the topographic isohypse (contour) lines, the area is not steeply sloped. There is no evidence of morphology associated with paleolandslides. Moreover, an apparent

right-lateral offset of the stoa in the sacred area is perpendicular to a steep slope. Thus, local geological and morphological conditions do not give impression of that site suitable for mass movement. It is more likely that the observed ruptures were associated with earthquake faulting on the Mugla Fault. In both cases, an assessment can be made about the potency of the related earthquake. Karabacak et al. (2013) formed a comparative scheme based on building damage and bedrock for EMS-98 (Grünthal 1998) and ESI-07 (Michetti et al. 2007) intensities reported from different archaeological sites in the world. Taking into account the overall damage and geological characteristic of Lagina in this scheme, we suggest that the deformation observed in the sacred area is the result of strong ground shaking with a considerable intensity.

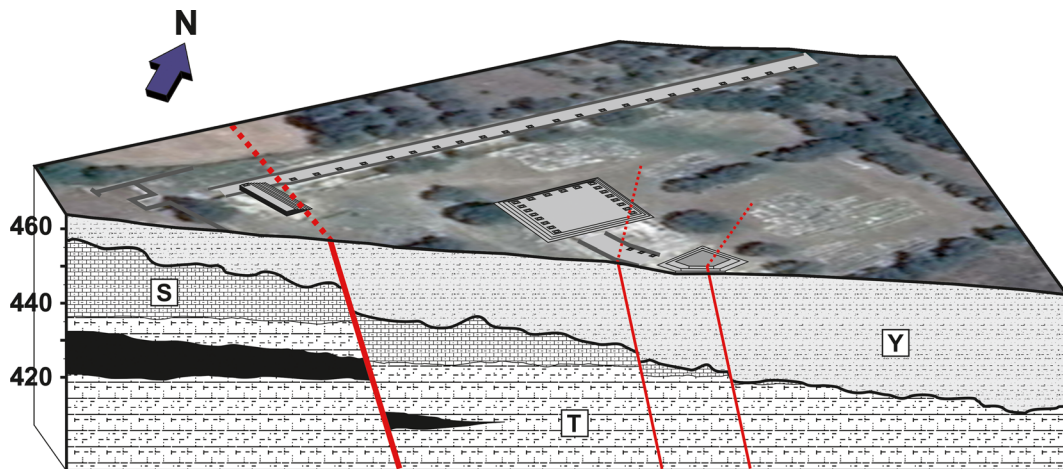


**Fig. 12** Three-dimensional model of the Lagina. It schematizes the underground geological characteristics of the sacred area. Surface image of the model is taken from Google Earth software. Terrain data is generated using the AsterGDEMv2. Geological background is compiled from previous studies (Becker-Platen 1970; Alcicek 2010; Güner et al. 2011; Kahraman et al. 2011) and simplified on the basis of author’s field observations (red lines show the faults). *T*

Turgut Formation, Middle Miocene lacustrine units (well bedded sand stone, siltstone, marn, clay stone, and lignite layers); *S* Sekkoy Formation, Middle Miocene lacustrine units (limestone and marn); *Y* Yatagan Formation, Upper Miocene-Pliocene lateral fan units with fluvial and lacustrine deposits (reddish conglomerate, sandstone, and mudstone with marn interlayered)

The results of dating the organic material and bone samples from the uppermost laminations in the covered sedimentary strata, which were immediately overlain by collapsed blocks, indicated calibrated ages between 220 and 405 AD (Table 1). TL dating of ceramic samples from similar overlaid levels present slightly before 4th *c.* AD, and it supports the radiocarbon results (Table 1). Thus, these age results suggest that the sacred area abruptly collapsed after 220 AD. Considering that the coseismic shaking damage is preserved to the present, it can be concluded that the sacred area could not have been used after destruction. It was probably abandoned. However, the youngest monumental structures of the Lagina sacred area were built in 325 AD. Thus, this situation realized that the sacred area must have collapsed in the 4th *c.* AD or slightly later. In this period, the Eastern Mediterranean experienced an unusual clustering of destructive earthquakes between the 4th *c.* and 6th *c.* AD (Pirazzoli et al. 1996). For example, a notable earthquake in Crete at this time that occurred on 21 July, 365 AD ( $M > 8$ ), destroyed nearly all settlements in the vicinity of the Aegean Sea and was followed by a tsunami (Guidoboni et al. 1994). Stiros (2001) suggests that the 365 AD earthquake was an exceptional event in the seismic history of the area, and it may have triggered the series of earthquakes that occurred during the period between the 4th *c.* and 6th *c.* AD. By implication, the earthquake that was responsible for the extensive destruction in the Lagina corresponds to one record of this period in the Karia.

The trend of the Mugla Fault extends obliquely to major normal fault systems of the western Anatolian extensional region. Data collected and evaluated as part of detailed field observations demonstrate that the Mugla Fault has strike-slip component and an important role in terms of earthquake faulting. There are numerous subsidiary faults representing strike-slip components aligned obliquely to major normal fault systems, and their recent behaviors are not as well documented as the neighboring major active faults. Considering the trend of the Mugla Fault, it can be concluded that subsidiary faults representing strike-slip component are active and render an important role in the seismicity of the western Anatolian extensional region.

## 5 Conclusions

The Mugla Fault is a NW-SE trending fault zone, and it is obliquely situated in the western Anatolia extension region. There are different interpretations on the sense of the

motion and activity of the fault in previous studies. The location of the Mugla Fault in the center of the Karia region provides excellent opportunities for the interpretation of the fault's characteristics. The 2000-year-old ruins of the Lagina sacred area are cut by fractures of tectonic origin that were probably associated with an earthquake on Mugla Fault in the 4th *c.* AD or slightly later. Archaeoseismological analysis of the sacred area with supporting geological and geomorphological observations indicates that there was Holocene activity of the Mugla Fault, and documented field evidence suggests that the dominant motion along the fault was dip-slip with a dextral strike-slip component. Thus, this study reveals that the subsidiary faults aligned obliquely to major normal fault systems in western Anatolia have strike-slip components and may be associated with a significant portion of the recent extensional dynamics.

**Acknowledgments** The first fieldwork for this study was conducted in May 2009 at the site. It was completed in January 2015 with the sampling. Dating of the samples was funded by the Eskisehir Osmangazi University Research Foundation (project no: 2014-534). Radiocarbon analyses were performed in the Beta Analytic Radiocarbon Dating Laboratory. Thermoluminescence analyses were performed in the laboratory of the Institute of Nuclear Science (Ankara University). Special thanks go to Dr. Sevgi Altınok (Eskisehir Osmangazi University) for her comments on an earlier version of this manuscript. The author is grateful to the journal editors and two anonymous reviewers for their comments, which improved the manuscript.

## References

- Alcicek H (2010) Stratigraphic correlation of the Neogene basins in southwestern Anatolia: regional palaeogeographical, palaeoclimatic and tectonic implications. *Palaeogeogr Palaeoclimatol Palaeoecol* 291:297–318
- Ambraseys NN, Finkel CF (1987) The Saros-Marmara earthquake of 9 August 1912. *Earthq Eng Struct Dyn* 15:189–211
- Ambraseys NN, Jackson JA (1998) Faulting associated with historical and recent earthquakes in the Eastern Mediterranean region. *Geophys J Int* 133:390–406
- Barka AA, Altınok E, Akyüz S, Şaroğlu F, Emre Ö, Kuşçu İ (1996) Güneybatı Anadolu'nun aktif fayları ve kireçtaşı fay sevelerinin incelenmesi (Investigations of active faults and limestone scarps in SW Anatolia). TÜBİTAK (YDABÇAG-237/G) Project Report, Ankara.
- Becker-Platen JD (1970) Lithostratigraphische Untersuchungen im Kanozoikum Südwest Anatoliens (Türkei) –Kanozoikum und Braunkohlen der Türkei, Beiheft. *Geol Jahrb* 97:1–244
- Bottari C, Stiros SC, Teramo A (2009) Archaeological evidence for destructive earthquakes in Sicily between 400 B.C. and A.D. 600. *Geoarchaeology* 24:147–175. doi:10.1002/geo.20260

- Büyüközer A (2010) The rates which are applied in the infrastructure and stylobate settings of Lagina Hecate temple. Pamukkale University Journal of Social Science Institute 7:1–14
- Duman TY, Emre Ö, Özalp S, Elmacı H (2011) 1:250,000 scale active fault map series of Turkey, Aydın (NJ 35–11) Quadrangle. Serial Number: 7, General Directorate of Mineral Research and Exploration, Ankara-Turkey
- Ekici M (2010) Evaluation of coins found at Lagina Hecate sacred area. Pamukkale University Journal of Social Science Institute 7:31–38
- Ergin K, Güçlü U, Uz Z (1967) A catalogue of earthquakes for Turkey and surrounding area 11 AD to 1964 AD. ITU Earth Physics Institute Publications, Istanbul
- Eyidoğan H, Akıncı A, Gündoğdu O, Polat O, Kaypak B (1996) Gökova Havzasının güncel depremselliğinin incelenmesi (Investigation of recent seismicity of Gökova Basin). TÜBİTAK (YDABÇAG-238/G) Project Report, Ankara.
- Galadini F, Hinzen KG, Stiros S (2006) Archaeoseismology: methodological issues and procedure. *J Seismol* 10(4):395–414
- Grünthal G (ed) (1998) European macroseismic scale. European Seismological Commission, Sub-commission on Engineering Seismology, Working Group Macroseismic scales, Luxembourg, 99 pp
- Guidoboni E, Comastri A (2005) Catalogue of earthquakes and tsunamis in the Mediterranean area from the 11th to the 15th century. Istituto Nazionale di Geofisica e Vulcanologia
- Guidoboni E, Comastri A, Traina G (1994) Catalogue of ancient earthquakes in the Mediterranean area up to the 10th century. ING-SGA, Bologna
- Gürer ÖF, Özbüran M, Sangu E, Gürbüz AY (2011) Muğla Yatağan Havzası ve Çevresinin Neotektonik İncelenmesi (Neotectonic investigation of the Mugla-Yatagan Basins and surrounding area), TÜBİTAK (108Y277) Project Report, Ankara
- Hinzen KG (2009) Simulation of toppling columns in archaeoseismology. *Bull Seismol Soc Am* 99(5):2855–2875
- Kahraman B, Dirik K, Özsayın E, Kutluay A (2011) Tectonics of the Yatağan - Eskişehir Basin, western Anatolia, Turkey. 64th Geological Congress of Turkey, Abstract Book, p. 4.
- Karabacak V, Yönlü Ö, Dökü E, Kıyak NG, Altunel E, Özüdoğru Ş, Yalçınar ÇÇ, Akyüz HS (2013) Analysis of seismic deformations at the Kibyra Roman stadion. SW Turkey. *Geoarchaeology* 28:531–543
- Karcz I, Kafri U (1978) Evaluation of supposed archaeoseismic damage in Israel. *J Archaeol Sci* 5:237–253
- Keefer DK (1984) Landslides caused by earthquakes. *Geol Soc Am Bull* 95:406–421
- Marco S, Kamai R, Hatzor YH, Wechsler N, Katz O (2008) Constraining location and size of historical earthquakes using mechanical analyses of damaged archeological sites: examples from Dead Sea Fault. *European Seismological Commission ESC* 2008, 31st General Assembly, Crete, pp 7–12, September 2008
- Michetti AM, Esposito E et al (2007) In: Vittori E, Guerrieri L (eds) *Memorie Descrittive della Carta Geologica d'Italia, Environmental Seismic Intensity Scale 2007 – ESI 2007*, vol LXXIV. Servizio Geologico d'Italia, Dipartimento Difesa del Suolo, APAT, SystemCart Srl, Roma, pp 7–54
- Pirazzoli PA, Laborel J, Stiros SC (1996) Earthquake clustering in the Eastern Mediterranean during historical times. *J Geophys Res* 101(B3):6083–6097
- Şaroğlu F, Emre Ö, Boray A (1987) Türkiye'nin Diri Fayları ve Depremsellikleri (Active faults and seismicity of Turkey). General Directorate of Mineral Research and Exploration, Ankara, 394 p
- Şengör AMC, Görür N, Şaroğlu F (1985) Strike slip faulting and related basin formation in zones of tectonic escape: Turkey as a case study. Edited by K.T. Biddle and N. Christie, *Blick. SEPM Spec Publ* 37:227–264
- Soysal H, Sipahioğlu S, Kolçak D, Altınok Y (1981) Türkiye ve çevresinin deprem katalogu, MÖ 2100-MS 1900 (Earthquake catalogue of Turkey and surroundings, 2100 BC-1900 AD). TÜBİTAK Publications (No. TBAG 341), 99 p.
- Stiros SC (1996) Identification of earthquakes from archaeological data: methodology, criteria and limitations. In: Stiros, S.C. & Jones, R.E. (eds), *Archaeoseismology. Occasional Paper No. 7 of the Fitch Laboratory, British School at Athens*, 129–152.
- Stiros S (2001) The AD 365 Crete earthquake and possible seismic clustering during the 4–6th centuries AD in the Eastern Mediterranean: a review of historical and archaeological data. *J Struct Geol* 23:545–562
- Sümer Ö, İnci U, Sözbilir H (2013) Tectonic evolution of the Söke Basin: extension-dominated transtensional basin formation in western part of the Büyük Menderes Graben, Western Anatolia, Turkey. *J Geodyn* 65:148–175
- Tan O, Tapırdamaz MC, Yörük A (2008) The earthquake catalogues for Turkey. *Turk J Earth Sci* 17:405–418
- Tırpan AA (1997) Buluntular ışığında Lagina ve yakın çevresinin tarihi süreci (Historical process of Lagina and its surroundings in the light of findings). Selçuk University Faculty of Art and Science Journal 11:75–98
- Tırpan AA (2012) Lagina excavations 2011. Republic of Turkey Ministry of Culture and Tourism Publications
- Tırpan AA, Söğüt B (2003) Lagina Excavations 2002. Republic of Turkey Ministry of Culture and Tourism Publications, ISSN 1017–7655, Ankara, pp 87–100
- Tırpan AA, Söğüt B (2010) Lagina excavations 2008. Republic of Turkey Ministry of Culture and Tourism Publications, ISSN 1017–7655, Ankara, pp 505–527
- Uzel B, Sözbilir H, Özkaymak Ç (2012) Neotectonic evolution of an actively growing superimposed basin in Western Anatolia: the Inner Bay of İzmir, Turkey. *Turk J Earth Sci* 21:439–471